



Preparations and thermal properties of micro- and nano-BN dispersed HDPE composites

Jinwoo Jung, Jaewoo Kim*, Young Rang Uhm, Jae-Kyun Jeon, Sol Lee, Hi Min Lee, Chang Kyu Rhee

Nuclear Materials Research Division, Korea Atomic Energy Research Institute, 1045 Daedukdaero, Daejeon 305-353, Republic of Korea

ARTICLE INFO

Article history:

Received 25 May 2009

Received in revised form 24 August 2009

Accepted 18 October 2009

Available online 28 October 2009

Keywords:

Boron nitride

Nano-particles

HDPE nanocomposites

Thermal insulation

Neutron shield

ABSTRACT

The thermal properties of micro-sized boron nitride (BN) and nano-sized BN dispersed high density polyethylene (HDPE) composites were investigated by means of differential scanning calorimetry (DSC) and thermo-gravimetric analysis (TGA). Nano-BN powder was prepared by using a ball mill process before it was mixed in HDPE. To enhance the dispersivity of nano-BN in the polymer matrix, the surfaces of the nano-particles were treated with low density polyethylene (LDPE) which was dissolved in the cyclohexane solvent. The average particle sizes of micro-BN powder and LDPE coated nano-BN powder were $\sim 10\ \mu\text{m}$ and $\sim 100\ \text{nm}$ respectively. Dispersion and distribution of 5 wt% and 20 wt% of micro-BN and nano-BN respectively mixed in HDPE were observed by using the scanning electron microscope (SEM). According to the thermal analyses of pure HDPE, micro-BN/HDPE, and nano-BN/HDPE, 20 wt% nano-BN/HDPE composite shows the lowest enthalpy of fusion (ΔH_m) and better thermal conductive characteristics compared to the others.

© 2009 Elsevier B.V. All rights reserved.

1. Introduction

Polymer composites filled with inorganic or organic fillers could be widely used in the industries including electronics, packaging, medical and health cares, tools, and automobile, etc., due to their superior mechanical, thermal, optical, and electrical properties compared to those of pure polymeric materials [1–5]. Inorganic polymer composites have the advantages of the polymeric properties together with the characteristics of the inorganic particles. The homogeneous dispersion of the filler particles in the polymeric matrix may improve the material characteristics. For example, boron nitride (BN) and their polymer composites are especially important because of their superior electrical and thermal properties [6,7]. BN is a low atomic numbered nonmetallic compound; its melting temperature ($\sim 3000\ ^\circ\text{C}$) is very high so as to be used as thermal insulation. BN/polymer composites can decrease thermal expansion and increase thermal conductivity while enhancing the electrical insulation properties [8,9]. Also, the addition of a small amount of BN in polymers might enhance extrusion property by increasing their flowability [10]. More practically, BN can also be used as a thermal neutron absorber due to the boron atom's high thermal neutron absorption cross-section ($\sim 760b$,

$b = 10^{-24}\ \text{cm}^2$). Polyethylene (PE) mixed with a BN filler can be used as a shielding material for satellites from cosmic radiation while it has the superior thermal property and chemical stability [11,12].

It is, in general, known that the properties of an inorganic or organic filler dispersed polymer could be greatly enhanced when the fillers have the nanometer scales [13–17] while there are not many publications currently available related to the nano-sized BN particle reinforced polymer composites. There is a high tendency of agglomeration of the nano-particles due to its high surface energy when they are mixed in the polymeric matrix. This might be one of the major difficulties for the preparation of the polymer nanocomposites leading them to the unwanted thermal and mechanical properties [18,19]. In this respect, it is critical that the nano-particles must be uniformly dispersed within the polymer matrix to achieve the proper property enhancement. For homogeneous dispersion of nano-BN in HDPE in this study, we treated the surface of the nano-BN particles prepared by a ball mill process with low density polyethylene (LDPE) which was dissolved in the cyclohexane solvent at a certain temperature [20]. The characteristics of the prepared samples in each step were measured and observed by using various analytic tools including the particle size analyzer (PSA), Brunauer–Emmett–Teller (BET), X-ray diffraction (XRD), scanning electron microscope (SEM), and transmission electron microscope (TEM). We also explored the thermal characteristics of pure HDPE, micro-BN/HDPE, and nano-BN/HDPE

* Corresponding author. Tel.: +82 42 868 8906.

E-mail address: kimj@kaeri.re.kr (J. Kim).

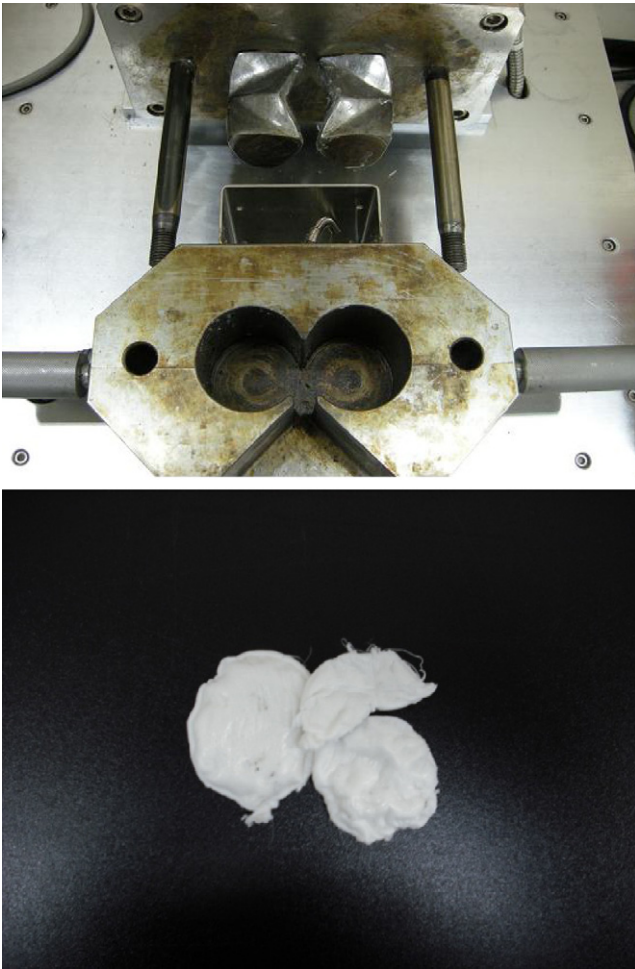


Fig. 1. Polymer melt mixing roller blades and produced nano-BN/HDPE composite.

composites by means of differential scanning calorimetry (DSC) and thermo-gravimetric analysis (TGA) in this investigation.

2. Experimental

2.1. Materials and mechanical activation (MA) process

High density polyethylene (SK Chemicals, ROK, >99%) and boron nitride powder (High Purity Chemicals, Japan, >99.0%, ca. $10\ \mu\text{m}$) were used as a polymer base and a filler respectively in this investigation. HDPE has the form of a pellet with a diameter which is $\sim 3\ \text{mm}$ whereas BN is a powder whose particle size is approximately $\sim 10\ \mu\text{m}$. In fact, the particle size distribution of BN was measured by the SEM images and was in between $5\ \mu\text{m}$ and $10\ \mu\text{m}$. Nano-BN was produced by the mechanical activation (MA) process without any catalyst using a planetary mill (Fritsch, Pulverisette 6). Milling balls used in the experiments were made of zirconia (ZrO_2); its diameter was 4 mm. The weight ratio between BN powder and zirconia balls was 1:10. The rotation speed of the disk and milling time were varied at 300–600 rpm and 1–72 h depending on the experimental conditions respectively. The milling jars were also made of zirconia the same as the balls. The morphologies of commercial micro-BN and the prepared nano-BN powders were observed by using FE-SEM (Sirion, FEI Netherlands) and FE-TEM (JEM-2100F, JEOL Ltd. Japan) and the size of the particles were measured and calculated by PSA (90Plus, Brookhaven Instruments Corp.) and BET (BEL 30RP-mini, BEL Japan Inc.) respectively.

2.2. Surface treatment of nano-BN

After micro-BN was pulverized by the milling process described in the previous section, the surface of the nano-BN powder was coated with LDPE which was dissolved in cyclohexane to increase the degree of dispersion of the nano-particles in the melted HDPE matrix. LDPE, as a surface treatment agent, was used because it is the same material as the HDPE base which can increase the wettability and lubricacy of the nano-particles in the polymer matrix. The miscibility of LDPE with linear polymers such as HDPE or linear low

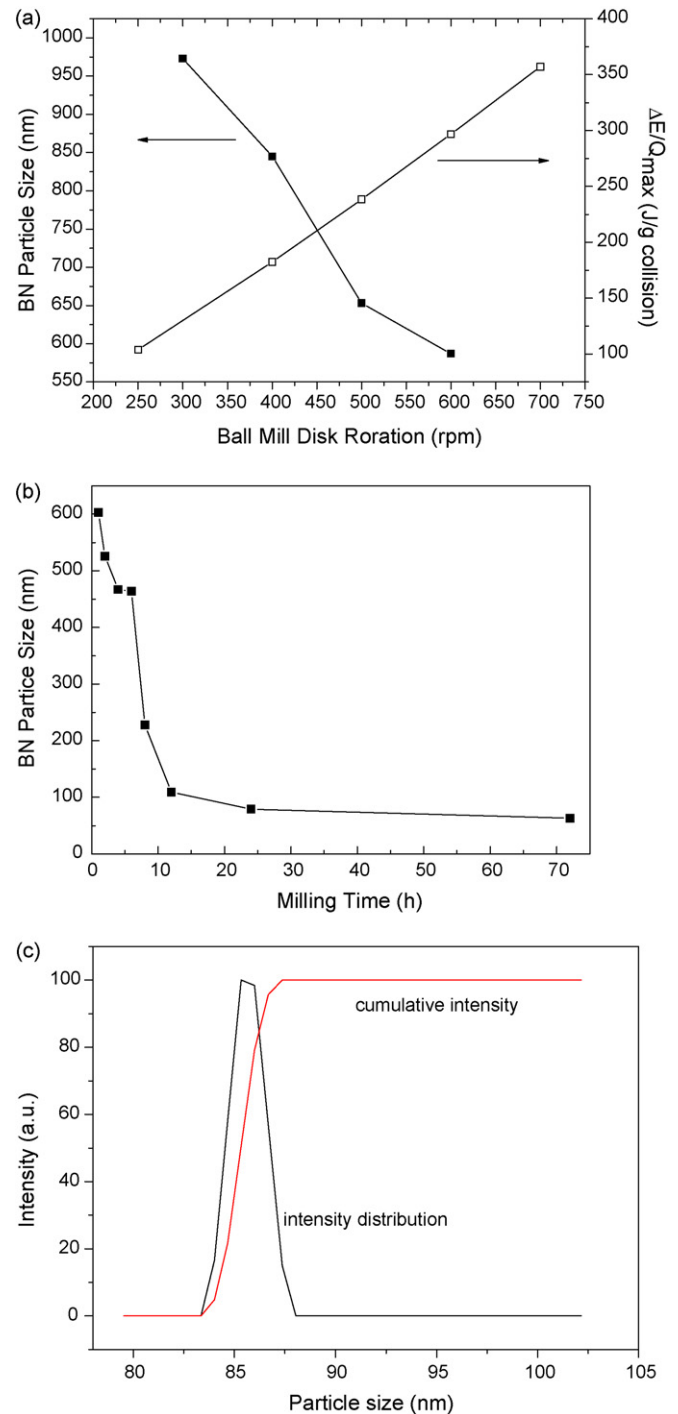


Fig. 2. Variances of BN particle sizes dependent on (a) ball mill disk speed and the transferred energy to powder, (b) milling time (ball to powder ratio = 10:1), and (c) typical size distribution of pulverized BN.

density polyethylene (LLDPE) is also demonstrated recently [21,22]. LDPE could be dissolved in the organic solvents such as toluene and cyclohexane while the latter shows the better LDPE solubility. 0.5 g of LDPE powder was dissolved in 100 ml of cyclohexane ($\sim 110^\circ\text{C}$) which was stirred magnetically on the hot plate. After the LDPE powder was completely dissolved in cyclohexane, 2 g of nano-BN was added. The stirring process was continued until the transparent LDPE dissolved solvent was changed to the white color of BN. In most cases, it took about 10 min for coating LDPE onto the nano-BN surface. It was then dried in the hood for more than 12 h to obtain the LDPE coated nano-BN powder.

2.3. Preparations of micro-BN/HDPE and nano-BN/HDPE

BN/HDPE composites were fabricated by mixing micro-BN and prepared LDPE coated nano-BN powders in the high polymer melt mixer (Eastern Engineering, Inc., ROK) as shown in Fig. 1(a). BN powder and HDPE pellets were pre-mixed homogeneously by using a powder mixer prior to being melted for mixing in the polymer mixer. The temperature of melted polymer was set at $\sim 170^\circ\text{C}$ and the rotation speed of the roller blades was 40 rpm. The weight concentrations of the powder in HDPE were 5 wt% and 20 wt% respectively for both micro- and nano-BN. Fig. 1(b) shows an example of 5 wt% nano-BN/HDPE composite which was obtained from the above mentioned mixing process.

2.4. Material property tests

To evaluate the morphological status and the degree of dispersion of the particles in the prepared samples, SEM and TEM images were obtained for micro-BN/HDPE and nano-BN/HDPE composites. The thermal properties of the samples were also evaluated by means of DSC and TGA. The DSC (TA Instrument DSC-Q100, USA)

samples were prepared by using a mechanical grinder to make the sample. Its weight was in the range from 5 mg to 6 mg. DSC was operated at the heating rate of $10^\circ\text{C}/\text{min}$ from 30°C to 200°C in a nitrogen environment so as to prevent the unwanted reactions of the samples with the oxygen at high temperature. The sample was then cooled to 30°C . TGA (TA Instrument SDT-Q600, USA) samples were also prepared at weights from 11 mg to 15 mg. TGA was operated at the heating rate of $10^\circ\text{C}/\text{min}$ from 30°C to 700°C in nitrogen environment the same as the DSC operation. From this data, the thermal characteristics of the samples such as melting temperature, enthalpy of fusion, crystallinity, and the degree of polymer decomposition were evaluated.

3. Results and discussion

3.1. Characteristics of prepared powders

To produce the nano-sized BN particles, micro-sized BN powder was pulverized by using a ball mill process. Under the various milling conditions, the size distributions of the BN particles produced were varied from $\sim 60\text{ nm}$ to $\sim 600\text{ nm}$ as shown in Fig. 2(a)–(c) taken by PSA. The prepared powder samples were ultrasonicated in an ethanol solvent for about 2 min prior to PSA measurements to enhance dispersion of the particles [23]. Agglomeration between particles in solvent was not severe during measurements and unimodal particle size distribution was also observed when using non-negatively constrained least squares multimodal size distribution function. Mean particle size of each sample was determined by averaging the mean values obtained from five measurements with the highest sample quality (>8) respectively. Mean particle size was also confirmed by SEM images in Fig. 3. Fig. 2(a) shows the BN particle size variances dependent on ball mill disk rotation speed from 300 rpm to 600 rpm

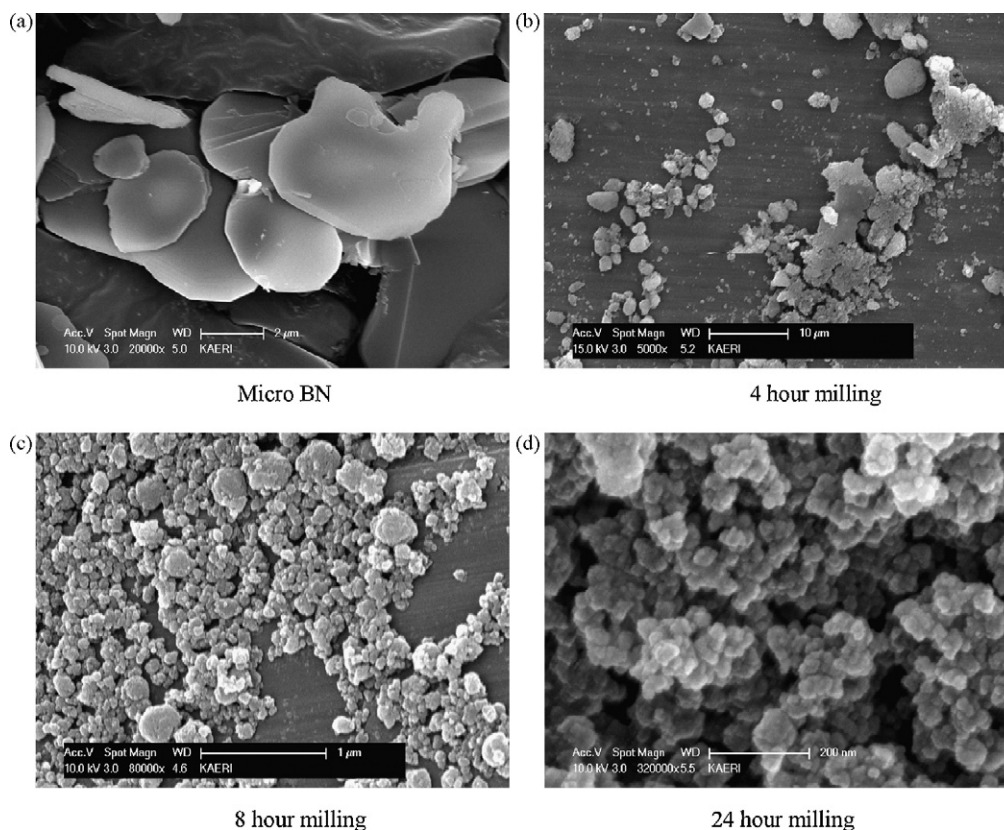


Fig. 3. The SEM images of BN dependent on the milling time at 600 rpm. (a) Micro-BN, (b) 4 h milling, (c) 8 h milling, and (d) 24 h milling.

during 1 h milling with the ratio of zirconia ball to powder of 10:1 and the transferred energy to powder per milling ball and per collision. As it can be expected, the size of the BN particles was reduced from $\sim 1 \mu\text{m}$ at 300 rpm to $\sim 600 \text{ nm}$ at 600 rpm, i.e. more energy was delivered to the particles per unit time for higher disk rotation. According to the Magini's model which estimates the transferred energy to powder per milling ball and per collision [24], $\Delta E/Q_{\text{max}}$ could be calculated as shown in Fig. 2(a), where ΔE is the transferred energy and Q_{max} is the maximum quantity of trapped material. The graph shows that the energy transferred to the powder increases as the disk rotation speed increases. Under the 600 rpm disk rotation speed, the size of the BN particles was decreased from 600 nm to 60 nm as the milling time was increased from 1 h to 72 h respectively as shown in Fig. 2(b). The graph indicates that the size of the BN particles is steeply diminished until the milling time reaches 10 h. Further pulverization however was not efficient even after 24 h milling for BN under the given conditions. It was determined that the optimum particle size of nano-BN was $\sim 80 \text{ nm}$ for 24 milling time with 600 rpm disk rotation. Typical particle size distribution of pulverized BN at 600 rpm during 24 h is shown in Fig. 2(c). Morphologies of BN powders obtained from the MA milling process dependent on the milling time are shown in SEM images in Fig. 3. Micro-BN which has no milling process involved shows the size of about $10 \mu\text{m}$ as mentioned earlier, whereas the others which are 4 h, 8 h, and 24 h milling processed at 600 rpm show the similar size distributions with the ones measured by PSA which are $\sim 460 \text{ nm}$, $\sim 230 \text{ nm}$, and $\sim 80 \text{ nm}$ respectively.

The nano-BN particles obtained from the milling process under 600 rpm and 24 h milling time were then surface treated with LDPE which was dissolved in cyclohexane at $\sim 110^\circ\text{C}$. To evaluate the LDPE coating status of the nano-BN particles, XRD patterns and TEM images were obtained as shown in Figs. 4 and 5 respectively. Fig. 4 shows the X-ray diffraction patterns for micro-BN, pure LDPE, LDPE coated nano-BN, and ZrO_2 . Main XRD peaks for ZrO_2 shown in Fig. 4 were obtained from Ref. [25]. Based on the XRD patterns, it was observed that the peaks for LDPE are disappeared because the amorphous phase was generated from the semi-crystalline structure of LDPE and the peaks for BN are lowered and broadened due to the LDPE coat on the nano-BN surface. It is clearly shown that the nano-BN particles are coated with LDPE from these patterns. The X-ray diffraction pattern for LDPE coated nano-BN also shows some ZrO_2 impurity generated during the milling process. The concentration of ZrO_2 impurity was also estimated by inductively coupled plasma-atomic emission spectrometry (ICP-AES) for pulverized BN powder prepared at 600 rpm during 24 h which is about 163 ppm. This impurity might be strongly dependent on the operational conditions such as the milling time and disk rotation speed. Also the TEM images in Fig. 5 show that the nano-BN particles are coated with LDPE. Their sizes are about $\sim 100 \text{ nm}$ which was increased from $\sim 80 \text{ nm}$ from the bare nano-BN particles. Consequently, the surface treatment process we developed in this investigation could be applied efficiently to the coating of inorganic or organic fillers using the organic compounds or various polymers which are same or similar to the base matrix.

3.2. Micro-BN/HDPE and nano-BN/HDPE composites

HDPE composites with the surface treated nano-BN powders were fabricated by using a polymer melt mixer with roller blades shown in Fig. 1(a). HDPE temperature was set at $\sim 170^\circ\text{C}$. Fig. 6 shows the SEM image for the status of dispersion for both (a and b) micro-BN particles (5 wt%) and (c and d) nano-BN particles (5 wt%) in HDPE matrix produced from polymer melt mixing. The size of micro-BN particles shown in the images (a) and (b) are bigger than $\sim 20 \mu\text{m}$ while the sizes of nano-BN particles in (c) and (d) are in

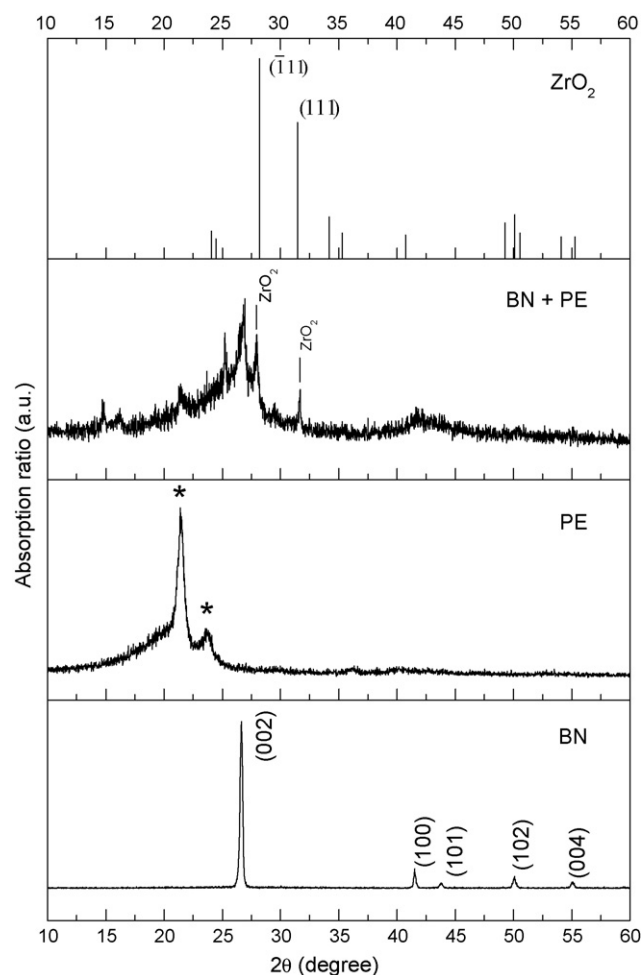


Fig. 4. X-ray diffraction patterns for micro-BN, pure LDPE, LDPE coated nano-BN, and ZrO_2 (* indicates the semi-crystalline structure of LDPE and LDPE coated nano-BN contains some zirconia impurities generated from the milling process).

between 100 and 200 nm. This indicates an agglomeration of particles may occur for those particles whose surfaces are not treated by the wetting agents enhancing their wettability and lubricacy. Some experiments report the different properties between the polymer composites of the surface treated or untreated particles whose sizes are the same [26,27]. This may be caused by either the agglomeration of the particles for surface untreated particles or impurities of surface treatment agents such as a series of silanes and stearic acid. However, only size effects must be considered in this investigation since the same material as the base matrix is used as a surface treatment catalyst.

3.3. DSC/TGA tests

Melting patterns by the endothermic heating process of pure HDPE, micro-BN/HDPE, and nano-BN/HDPE composites were evaluated by means of DSC measurements. From the DSC curves shown in Fig. 7, the endothermic parameters of each prepared sample were obtained. The melting temperature (T_m), the enthalpy of fusion (ΔH_m), and the degree of crystallinity (X_c) for each sample are listed in Table 1. The degree of crystallinity X_c of the prepared composites compared to pure HDPE was calculated using the equation $X_c = \Delta H_m(T_m)/\Delta H_m(T_m)$ where $\Delta H_m(T_m)$ is the enthalpy of fusion measured at the melting point for the prepared composites and $\Delta H_m(T_m)$ is the enthalpy of fusion measured at the melting point for pure HDPE obtained from the second heating process [28].

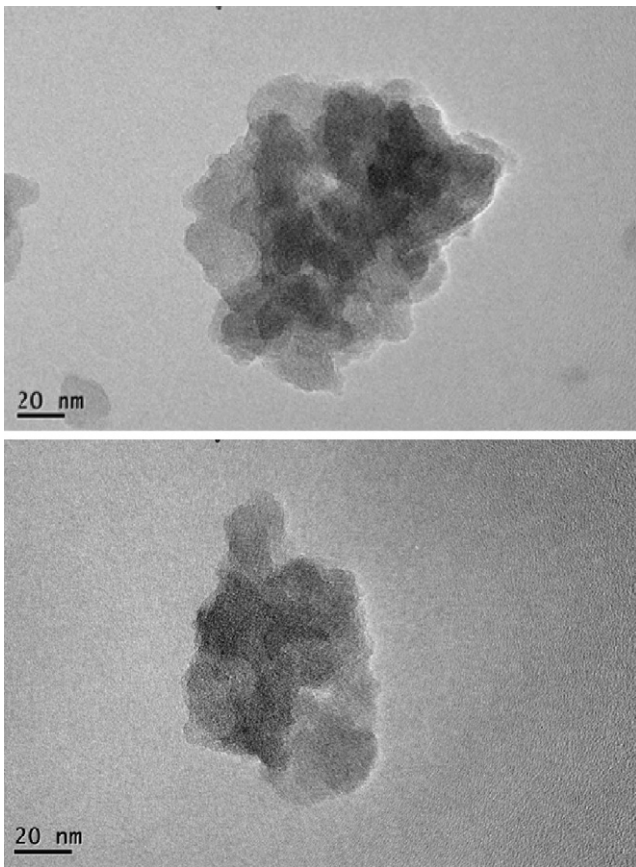


Fig. 5. TEM images of LDPE coated nano-BNs at 600 rpm.

Table 1

DSC thermal parameters for the pure HDPE, micro-BN/HDPE, and nano-BN/HDPE composites.

Materials	T_m ($^{\circ}\text{C}$)	ΔH_m (J/g)	X_c
Pure HDPE	138.3	181.2	1
Micro-BN/HDPE (5 wt%)	140.3	180.3	0.995
Micro-BN/HDPE (20 wt%)	139.1	139.2	0.768
Nano-BN/HDPE (5 wt%)	138.4	140.5	0.775
Nano-BN/HDPE (20 wt%)	139.9	118.7	0.665

According to Fig. 7 and Table 1, enthalpy of fusion for 20 wt% nano-BN/HDPE 118.7 J/g is the lowest among other samples while 5 wt% micro-BN/HDPE shows the highest enthalpy of fusion 180.3 J/g and 5 wt% nano-BN/HDPE presents a similar enthalpy of fusion with 20 wt% micro-BN/HDPE. On the other hand, melting points were about the same as $\sim 140^{\circ}\text{C}$ for most samples including pure HDPE. It can be assumed that 20 wt% nano-BN/HDPE shows the better thermal conductive characteristics possessing more thermal stability at the same temperature since the construction of the thermal conductive chains by the smaller BN particles can be easier than those by the larger BN particles [8]. The reason for similar melting points for the BN filler dispersed HDPE can be explained by the flexibility of polymer chains which are similarly maintained even when the fillers are dispersed in the polymer matrix. The thermal analyses for nano-sized calcium carbonate dispersed HDPE also shows the same results as the present investigation [15].

The TGA curves in Fig. 8 show T_5 (temperature at which 5 wt% loss occurs) and T_{max} (temperature at the maximum weight loss rate) for each prepared polymer composites. The TG curves imply the thermal stability of the prepared composites by showing the material decomposition characteristics. According to Table 2, pure HDPE shows the lowest $T_5 \sim 410.5^{\circ}\text{C}$ and $T_m \sim 467.2^{\circ}\text{C}$ while the material residue is zero at 550°C . On the other hand, BN dispersed HDPE composites show higher T_5 and T_m compared to

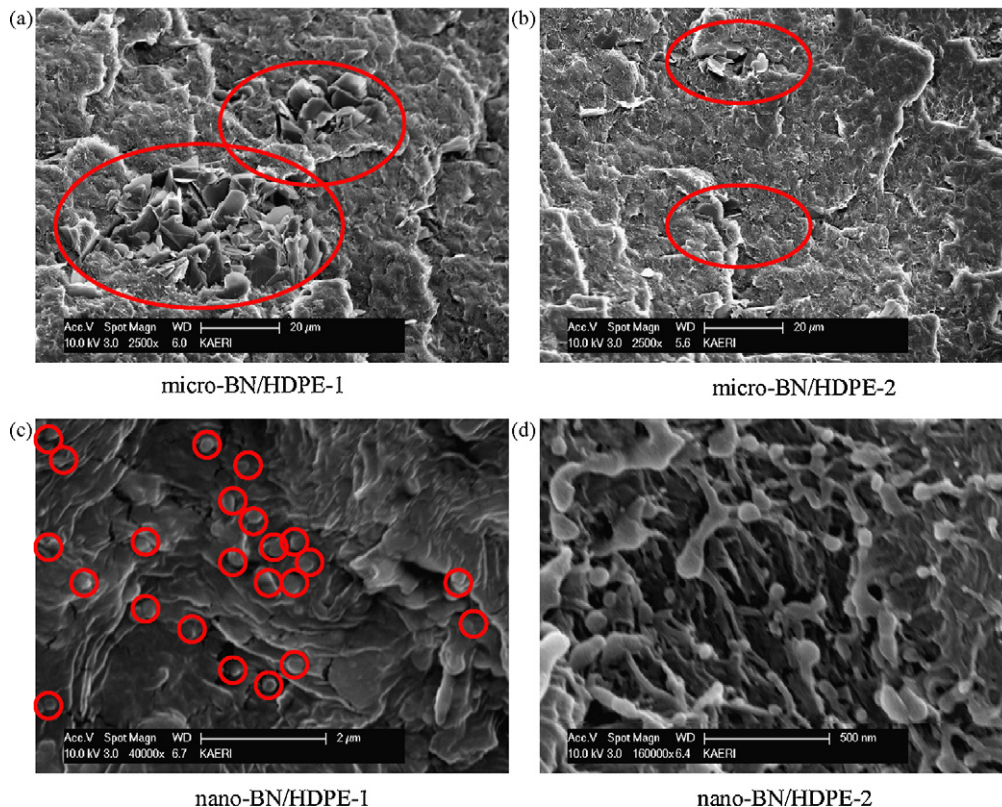


Fig. 6. SEM images for micro-BN and nano-BN particle in HDPE matrix ((a) micro-BN/HDPE-1, (b) micro-BN/HDPE-2, (c) nano-BN/HDPE-1, and (d) nano-BN/HDPE-2).

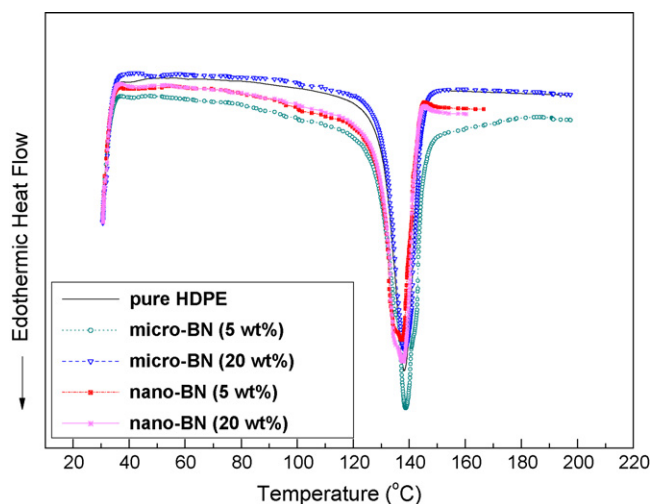


Fig. 7. Differential scanning calorimetry (DSC) thermogram for the pure HDPE, micro-BN/HDPE, and nano-BN/HDPE composites.

those for pure HDPE. Under the same wt% of BN, nano-BN/HDPE composite shows higher T_5 than micro-BN with 5 wt% whereas micro-BN/HDPE shows higher T_5 for 20 wt% BN while T_m for BN/HDPE composites is similar regardless of the weight concentration and the size of the fillers as shown in Table 2. However, it could be best assumed from the measured T_5 and T_m that 5 wt% nano-BN

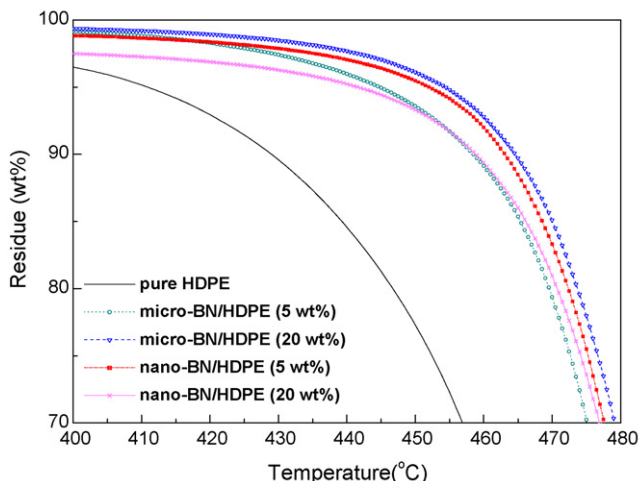
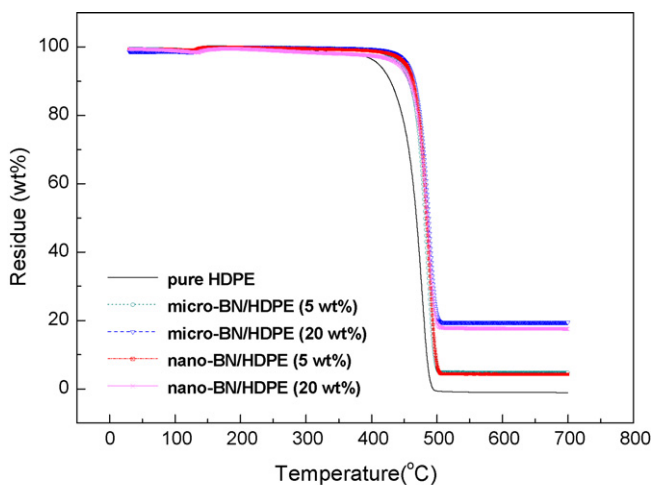


Fig. 8. TGA curves for pure HDPE, micro-BN/HDPE, and nano-BN/HDPE composites.

Table 2

TGA parameters of pure HDPE, micro-BN/HDPE, and nano-BN/HDPE composites.

Materials	T_5 (°C)	T_{max} (°C)	Residues (%)
Pure HDPE	410.50	467.2	0.0
Micro-BN/HDPE (5 wt%)	440.50	478.6	5.27
Micro-BN/HDPE (20 wt%)	454.00	482.5	20.93
Nano-BN/HDPE (5 wt%)	452.00	486.0	4.93
Nano-BN/HDPE (20 wt%)	441.50	483.4	18.11

dispersed HDPE shows the highest thermal decomposition stability compared to the others.

4. Conclusion

Nano-sized BN powder was successfully prepared by pulverizing micro-sized BN powder using a ball mill process without any wetting agents. To enhance the dispersivity of nano-BN in the polymer matrix, the surfaces of the nano-particles were treated with LDPE which was dissolved in the cyclohexane solvent. By means of the various analytic tools including PSA, TEM, and XRD, the size distribution of nano-BN powder under the various experimental conditions as well as the status of LDPE coating on the surface of nano-BN particles was evaluated. Surface treated nano-BN was mixed homogeneously in HDPE by using a polymer melt mixer while some agglomerations of the untreated micro-BN particles in HDPE were observed. 20 wt% nano-BN dispersed HDPE shows the lowest enthalpy of fusion having the highest thermal conductive characteristics among other prepared samples while the melting temperature and decomposition characteristics were similar. In this investigation, the preparation of nano-sized BN dispersed HDPE was successfully performed by using an organic-solvent surface treatment method together with a polymer melt mixing process and the highly enhanced thermal conductive characteristics for the nano-BN/HDPE composites were also observed. This type of polymer nanocomposite could be used as a neutron shield for satellite which needs lighter materials and also whose outer environments are extreme.

Acknowledgement

This work was supported by a Nuclear Energy R&D Program (Grant No. R-2007-3-155) sponsored by the Ministry of Knowledge Economy in the Republic of Korea.

References

- [1] M. Alexandre, P. Dubois, Mater. Sci. Eng. 28 (2000) 1–63.
- [2] A.S. Luyt, J.A. Molefi, H. Krump, Polym. Degrad. Stabil. 91 (2006) 1629–1636.
- [3] Z. Han, J.W. Wood, H. Herman, C. Zhang, G.C. Stevens, IEEE Int. Symp. Electr. Insul. (2008) 497–501.
- [4] L.C. Sim, S.R. Ramanan, H. Ismail, K.N. Seetharamu, T.J. Goh, Thermochim. Acta 430 (2005) 155–165.
- [5] W. Zhou, D. Yu, C. Min, Y. Fu, X. Guo, J. Appl. Polym. Sci. 112 (2009) 1695–1703.
- [6] G. Postole, M. Caldararu, N.I. Ionescu, B. Bonnetot, A. Auroux, C. Guimon, Thermochim. Acta 434 (2005) 150–157.
- [7] T. Jiang, Z. Jin, J. Yang, G. Qiao, J. Mater. Process. Technol. 209 (2009) 561–571.
- [8] W. Zhou, S. Qi, H. Li, S. Shao, Thermochim. Acta 452 (2007) 36–42.
- [9] W. Zhou, S. Qi, Q. An, H. Zhao, N. Liu, Mater. Res. Bull. 42 (2007) 1863–1873.
- [10] E.E. Rosenbaum, S.K. Randa, S.G. Hatzikiriakos, C.W. Stewart, D.L. Henry, M. Buckmaster, Polym. Eng. Sci. 40 (2000) 179–190.
- [11] C. Harrison, S. Weaver, C. Bertelsen, E. Burgett, N. Hertel, E. Grulke, J. Appl. Polym. Sci. 109 (2008) 2529–2538.
- [12] J. Yu, T.Y. Chen, R.G. Elliman, M. Petracic, Adv. Mater. 18 (2006) 2157–2160.
- [13] K. Chrissafis, K.M. Paraskevopoulos, E. Pavlidou, D. Bikiaris, Thermochim. Acta 485 (2009) 65–71.
- [14] N. Garcia, M. Hoyos, J. Guzman, P. Tiemblo, Polym. Degrad. Stabil. 94 (2009) 34–48.
- [15] S. Sahebian, S.M. Zebarjad, J.V. Khaki, S.A. Sajjadi, J. Mater. Process. Technol. 209 (2009) 1310–1317.
- [16] C.S. Reddy, C.K. Das, Compos. Interface 11 (2005) 687–699.
- [17] Q. Jiasheng, H. Pingsheng, J. Mater. Sci. 38 (2003) 2299–2304.
- [18] B.A. Rozenberg, R. Tenne, Prog. Polym. Sci. 33 (2008) 40–112.

- [19] A.P. Kumar, D. Depan, N.S. Tomer, R.P. Singh, *Prog. Polym. Sci.* 34 (2009) 479–515.
- [20] J.H. Kim, H.J. Oh, N.H. Lee, C.R. YOON, S.J. Kim, W.W. Kim, J.S. Song, *J. Korean Phys. Soc.* 48 (2006) 1329–1333.
- [21] O.D. Velazquez, S.G. Hatzikiriakos, M. Sentmanat, *J. Polym. Sci. Polym. Phys.* 46 (2008) 1669–1683.
- [22] O.D. Velazquez, S.G. Hatzikiriakos, M. Sentmanat, *Rheol. Acta* 47 (2008) 19–31.
- [23] N. Mandzy, E. Grulke, T. Druffel, *Powder Technol.* 160 (2005) 121–126.
- [24] M. Magini, A. Iasonna, F. Padella, *Scripta Mater.* 34 (1996) 13–19.
- [25] H.F. McMurdie, M.C. Morris, E.H. Evans, B. Paretzkin, W. Wong-Ng, C.R. Hubbard, *Powder Diffr.* 1 (1986) 265–275.
- [26] Z. Han, H. Pan, L. Dong, X. Zhang, 2008 Int. Sym. Electr. Insul., September 7–11, 2008.
- [27] Z. Han, C. Diao, Y. Li, H. Zhao, 2006 Annu. Rep. Conf. Electr. Insul. Dielectr. Phenom., 2006.
- [28] Y. Kong, J.N. Hay, *Polymer* 43 (2002) 3873–3878.